The young open cluster Markarian 50

Gustavo Baume,[1,2]★ Rubén A. Vázquez[2]★ and Giovanni Carraro[1,3]★

[1]*Dipartimento di Astronomia, Università di Padova, Vicolo Osservatorio 2, I-35122 Padova, Italy*
[2]*Facultad de Ciencias Astronómicas y Geofísicas de laUNLP, IALP-CONICET, Paseo del Bosque s/n, La Plata, Argentina*
[3]*Departamento de Astronomía, Universidad de Chile, Casilla 36-D, Santiago, Chile*

ABSTRACT

We report on a deep CCD $UBV(RI)_C$ photometric survey in the region of the young open cluster Markarian 50. The new photometric data allow us to extend the cluster membership down to $V \approx 17.5$, about 2 mag deeper than any previous investigation. On the basis of these data we derive a distance $d = 3460 \pm 350$ pc ($V_O - M_V = 12.7 \pm 0.2$), which turns out to be only slightly lower than previous estimates. The cluster presents differential reddening, with $E(B-V)$ values ranging from 0.69 to 1.1. The brightest member (HD 219460) is a double star, which we separate photometrically for the first time, providing individual magnitudes and colours for each component. One of them is a Wolf–Rayet (WR) star and, according to evolutionary models, the mass of its progenitor should be greater than $\sim$20 M$_\odot$. The age obtained for the cluster is 7.5 ± 2 Myr and the mass function for the most massive stars ($M > 1$ M$_\odot$) presents a slope $x \approx 1.0$.

Key words: stars: imaging – stars: individual: HD 219460 – stars: individual: WR 157 – stars: luminosity function, mass function – stars: Wolf–Rayet – open clusters and associations: individual: Markarian 50.

1 INTRODUCTION

Markarian 50 = OCL 257 = C2313 + 602 ($l = 111.36°$, $b = -0.20°$) is a compact group of stars associated with the northern part of the H II region Sharpless 157 (SG 13). This H II region (see Fig. 1) is mainly excited by the brightest stars of the cluster and partially by its surrounding association Cas OB2 (Lozinskaya, Sitnik & Lomovskii 1986). The cluster is placed in a direction where, according to Neckel & Klare (1980), the absorption rises even close to the Sun, reaching 2.5–3 mag in the first $\sim$500 pc. Markarian 50's brightest member is HD 219460, a close double star composed of a B-type star and a Wolf–Rayet (WR) type star.

The first attempt to derive the cluster basic parameters was carried out by Grubissich (1965) by means of *UBV* photographic photometry. Later on, Crampton (1975) performed spectroscopic measurements of the brightest stars. However, the first detailed photometric study was carried out by Turner et al. (1983), who obtained photoelectric photometry of 19 bright stars and spectroscopic observations of HD 219460. Finally, Massey, DeGioia-Eastwood & Waterhouse (2001) presented new spectroscopic data for the brightest stars in this object in a general study of WR stars in galactic open clusters and associations. All these studies provide information only on the brightest members of the cluster, but all of them basically point out that Markarian 50 stars suffer from a significant differential reddening and that the cluster apparently exhibits a nucleus/halo structure.

The present study is aimed at providing the first uniform and deep CCD photometric study of Markarian 50. These data will allow us to better probe the cluster fundamental parameters such as reddening, distance, size and age as established by Turner et al. on a more extended and deep data set. Besides, we will obtain the first estimate of the cluster luminosity function (LF) and initial mass function (IMF), which are very useful tools to understand the stellar formation process and modes over the whole Galactic disc (e.g. Miller & Scalo 1979; Will, Bomans & de Boer 1995; Scalo 1998).

The paper is organized as follows. In Section 2 we describe the observations carried out and the applied reduction procedure. In Section 3 we detail the data analysis including the cluster angular radius computation, membership assignments, HD 219460 parameters and the IMF derivation. Finally, in Section 4 we include a brief discussion and summarize our main findings.

2 OBSERVATIONS AND DATA REDUCTION

We performed CCD $UBV(RI)_C$ photometry of more than 1000 stars in the region of the open cluster Markarian 50 on 2002 November 11. The data were obtained using the Asiago Faint Object Spectrograph and Camera (AFOSC) that samples a 8.14×8.14 arcmin^2 field in a $1K \times 1K$ nitrogen-cooled thinned CCD, attached to the 1.82-m Copernico telescope of Cima Ekar (Asiago, Italy). The typical seeing value during the observing run was $\sim$2.0 arcsec. A description

★E-mail: gbaume@fcaglp.unlp.edu.ar (GB); rvazquez@fcaglp.unlp.edu.ar (RAV); giovanni.carraro@unipd.it (GC)
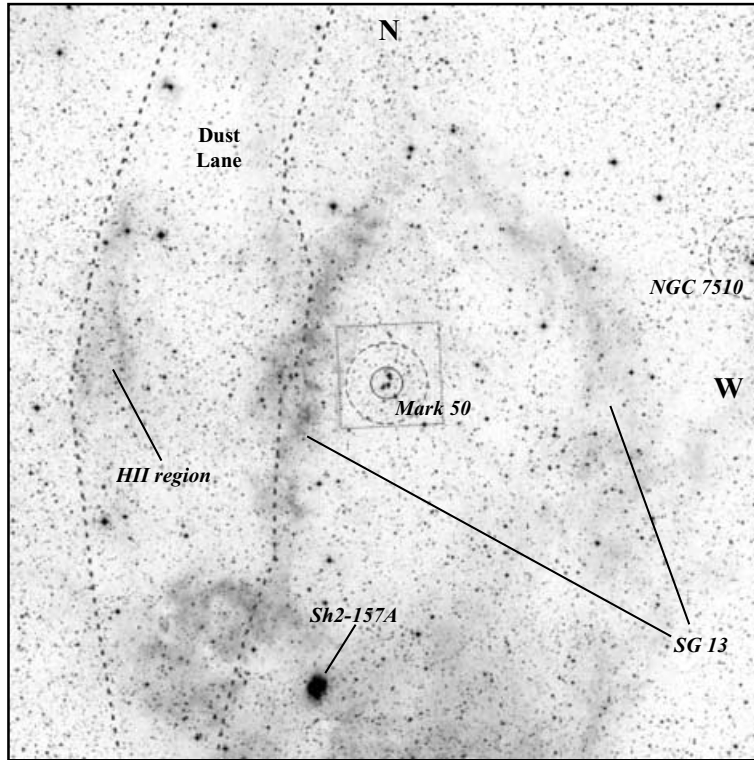
Figure 1. DSS-2 red filter image of Cas OB2 region (1 × 1 deg^2) centred on the open cluster Markarian 50. Main structures are indicated (Lozinskaya et al. 1986).

Table 1. Journal of observations of Markarian 50 and standard star field together with used calibration coefficients (2002 November 11).

Field	Exposure times (s)				
	U	B	V	R	I
Markarian 50	1200 × 2	800	600	400	400
	200	150	60	400	400
	–	15	5	5	5
PG 0231 + 051 (×3)	800	200	100	100	100

Calibration and extinction coefficients

$u_1 = +3.697 \pm 0.030$	$v_{1vi} = +0.926 \pm 0.024$
$u_2 = -0.187 \pm 0.038$	$v_{2vi} = -0.035 \pm 0.020$
$u_3 = +0.58$	$v_3 = +0.16$
$b_1 = +1.490 \pm 0.015$	$r_1 = +0.986 \pm 0.030$
$b_2 = +0.049 \pm 0.017$	$r_2 = -0.005 \pm 0.050$
$b_3 = +0.29$	$r_3 = +0.12$
$v_{1bv} = +0.912 \pm 0.017$	$i_1 = +1.592 \pm 0.066$
$v_{2bv} = -0.029 \pm 0.019$	$i_2 = +0.058 \pm 0.054$
	$i_3 = +0.08$

of the observed fields and exposure times can be found in Table 1. Fig. 2 shows the finding chart of the area of Markarian 50.

Data have been reduced with the IRAF packages CCDRED, DAOPHOT and PHOTCAL by using the point spread function (PSF) method (Stetson 1987). The calibration equations, obtained by observing the Landolt (1992) PG 0231 + 051 field twice before and once after the cluster observations, are

$$u = U + u_1 + u_2(U-B) + u_3X \quad (\text{rms} = 0.06) \tag{1}$$

$$b = B + b_1 + b_2(B-V) + b_3X \quad (\text{rms} = 0.03) \tag{2}$$

$$v = V + v_{1bv} + v_{2bv}(B-V) + v_3X \quad (\text{rms} = 0.02) \tag{3}$$

$$v = V + v_{1vi} + v_{2vi}(V-I) + v_3X \quad (\text{rms} = 0.02) \tag{4}$$

$$r = R + r_1 + r_2(V-R) + r_3X \quad (\text{rms} = 0.03) \tag{5}$$

$$i = I + i_1 + i_2(V-I) + i_3X \quad (\text{rms} = 0.04). \tag{6}$$

Here, *UBVRI* and *ubvri* are standard and instrumental magnitudes, respectively, and X is the airmass of the observation. The transformation coefficients and extinction coefficients for the Asiago Observatory (Desidera, Fantinel & Giro 2002) are shown at the bottom of Table 1. To obtain V magnitudes, we used expression (3) when the B magnitude was available; otherwise expression (4) was used. Fig. 3 shows the differences between our data and those of Turner et al. (1983) and Grubissich (1965) in the sense of 'our photometry minus theirs'. As shown in Table 2, the mean differences with data from Turner et al. (1983) are small but the standard deviations are however significant. The differences shown in Table 2 can potentially represent offsets of the present photometry and that of Turner et al. while, on the other hand, unresolved binary, fast rotators and/or variable stars can account for part of the high dispersion. Probably contributing to the high dispersion mention too is the fact that some CCD detectors can introduce systematic small errors, especially for stars where the maximum of the Balmer discontinuity appears as stated by Shorlin, Turner & Pedreros (2004). We cannot quantify the impact of this non-linear phenomenon on to our data, but it can partially explain the dispersion found for the $U–B$ index. A final comment has to do with the fact that the data of Turner et al. (1983)
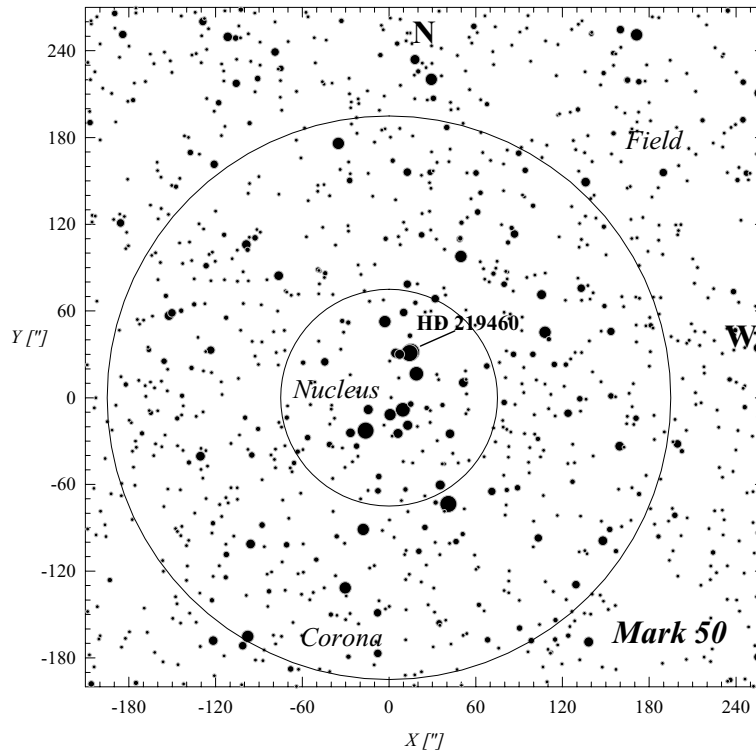
Figure 2. Finding chart of the area of Markarian 50 (*V* filter). The black solid circles, 1.25- and 3.25-arcmin radii, indicate the angular sizes found for the nucleus and the corona, respectively (see Section 3.1 and Fig. 4). For the coordinate reference system, the centre ($X = 0$; $Y = 0$) corresponds to $\alpha = 23^h15^m14\overset{s}{.}5$; $\delta = +60°26'30''\!.0$. *X–Y* units are arcsec.
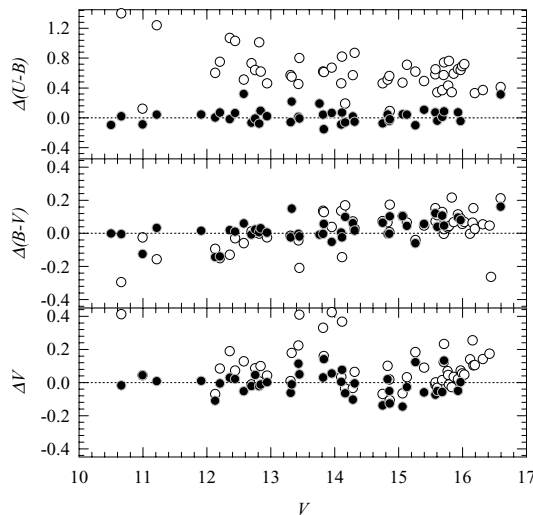
Figure 3. Comparison of our photometry with Turner et al. (1983, solid circles) and (Grubissich 1965, open circles).

are a combination of Kitt Peak photometry and differential photometry made at L. Figl Astrophysical Observatory of the University of Vienna. Therefore, we believe that the concluding explanation for the differences in Table 2 can be the combination of all the facts enumerated above.

As for the differences with the Grubissich (1965) data, the most remarkable shift appears in the ($U-B$) index, remaining quite high in the others. Fig. 3 indicates without any doubt that the problems come from the photographic photometry.

Table 2. Comparison of our photometry with that of Turner et al. (1983) and Grubissich (1965) in the sense of 'our data minus theirs'.

| Work	ΔV	$\Delta (B-V)$	$\Delta (U-B)$	N
Turner et al.	0.04 ± 0.19	0.02 ± 0.07	0.02 ± 0.10	43
Grubissich	0.11 ± 0.15	0.02 ± 0.11	0.61 ± 0.25	56

3 DATA ANALYSIS

3.1 Cluster angular radius

According to Dias et al. (2002) and Turner et al. (1983), Markarian 50 is an open cluster with a diameter of about 5 arcmin. Also, following Lyngå (1987), this cluster is of Trumpler class III 1 p (very strong concentration; most stars of nearly the same brightness; poorly populated).

Because our CCD observations cover the whole cluster surface and part of its surroundings (see Fig. 2), we decided to re-estimate the cluster size through star counts. To derive the radial stellar surface density, we first sought the highest peak in the stellar density to find the cluster centre. That peak was found at $\alpha_{2000} = 23^h15^m14\overset{s}{.}5$; $\delta_{2000} = +60°26'30''\!.0$ (see Fig. 2) not far from the centre positions given by Turner et al. (1983) or by Dias et al. (2002). The radial density profiles as shown in Fig. 4 have been constructed by performing star counts inside concentric annuli 0.5 arcmin wide around the cluster centre which were divided by their respective surfaces. Density profiles were constructed with our data (down to $V = 19$) and with the Second Generation Digitized Sky Survey (DSS-2) red image data down to a similar limiting magnitude. The same procedure was applied using Two-Micron All-Sky Survey (2MASS) data.
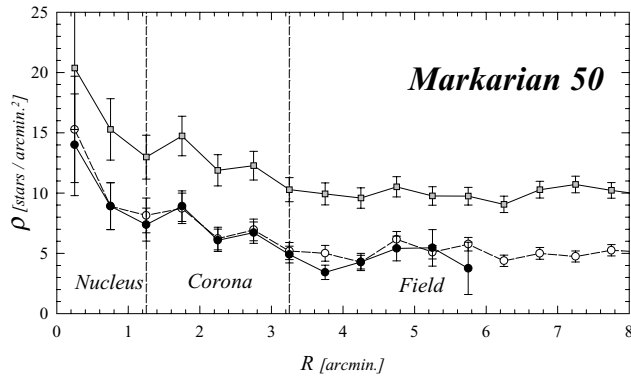
Figure 4. Density profiles in the region of Markarian 50 as a function of the radius. Filled circles indicate our data, open circles are data from the DSS-2 image and grey squares are 2MASS catalogue data. Dotted lines indicate the adopted limits for the cluster nucleus and corona.
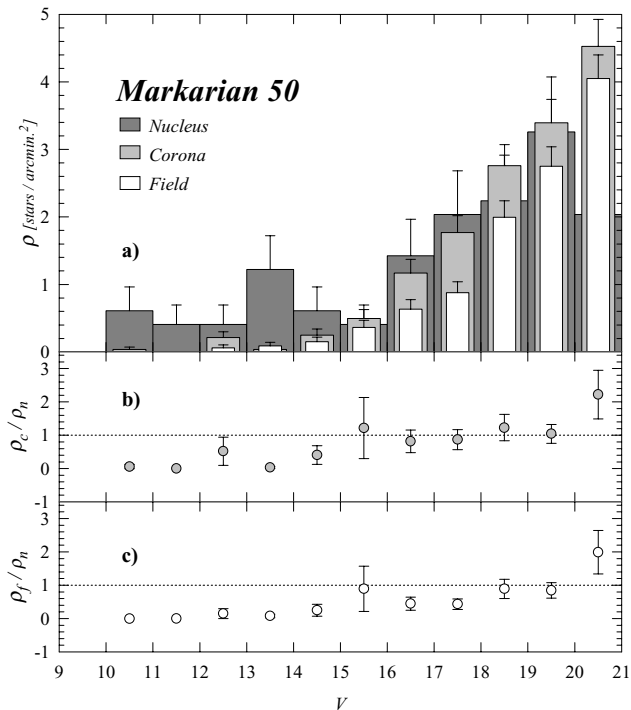
Figure 5. (a) Apparent LFs for the cluster nucleus, cluster corona and comparison field. (b) and (c) denote ρ_c/ρ_n and ρ_f/ρ_n as a function of V, respectively (see Section 3.1). Errors from Poisson statistics are also indicated.

Because beyond 3.5 arcmin from the cluster centre our data do not permit complete annuli, we have assumed that the observed portions are still representative of the field stellar populations around the cluster.

From the density profiles of Fig. 4 we can recognize three regions: (i) the cluster nucleus; (ii) a cluster corona (confirming the nucleus/corona structure previously suggested by Turner et al. 1983); (iii) the field surrounding it. We therefore adopt $r_n = 1.25$ arcmin and $r_c = 3.25$ arcmin for the nucleus and corona radii, respectively. Likewise, we notice that the radial profile from optical data seems to show statistical fluctuations larger than those from 2MASS data. This picture is completely coherent with that already stated by Turner et al. (1983) who, from their stellar counts outside the clus-

ter boundaries, interpreted the fluctuations as a consequence of the presence of patches of dust placed in the cluster direction.

On the other hand, when the respective apparent LFs are built for each region (Fig. 5a), Markarian 50 emerges clearly against the background star field leaving no doubt about its physical nature. The question emerges then about the type of stars that are present in the cluster corona. In this respect, we investigated the ratios between the number of stars found at similar V magnitude bins in the corona, ρ_c, the field, ρ_f, and the nuclear region, ρ_n (see Forbes 1996 for details). The results of the ratios ρ_c/ρ_n and ρ_f/ρ_n are shown in Figs 5(b) and (c), respectively. It is easily noticed that the ratio ρ_c/ρ_n is an increasing function. If we assume that the field stars keep the same distribution over the whole cluster surface, Fig. 5(b) indicates that the corona is richer in faint (less massive) stars than the cluster nucleus. Because of the extreme youth of Markarian 50, this feature is probably due to a primordial mass segregation effect and not a dynamical one. As expected, it appears that the ratio ρ_f/ρ_n shown in Fig. 5(c) is quite a flat function that just starts rising at $V \approx 18$ (see Table 4) exactly where the completeness corrections of our data become important. Additionally, both functions show a clear peak at $V = 15$–16 which, when connected to the luminosity distributions shown in Fig. 5(a), forces us to assume it is produced by a deficiency of this type of star in the nuclear region.

3.2 Photometric diagrams

Fig. 6 presents the colour–colour diagrams: $(U{-}B)$ versus $(B{-}V)$ and $(B{-}V)$ versus $(V{-}I)$. The former clearly shows that Markarian 50 suffers from differential reddening, whereas the latter gives only a marginal evidence that the ratio of total to selective absorption $[R = A_V/E(B{-}V)]$ could be larger than normal (see Section 3.4). A similar conclusion is obtained by using Caldwell et al. (1993) relations instead of Cousins (1978a), Cousins (1978b) relations.

Optical colour–magnitude diagrams (CMDs) are given in Fig. 7, while Fig. 8 shows the CMDs constructed from the 2MASS data. Because of obvious changes in the sensitivity of the CCD, all these CMDs extend downwards to different V_{lim} (from $\sim$18.5 in $U{-}B$ to $\sim$21.5 in $V{-}R$ and $V{-}I$).

In both Figs 7 and 8 we show the diagrams of the stars placed inside the cluster radius (see Section 3.1) together with the diagrams of the respective comparison fields indicated as comparison field 1 (CP1) and comparison field 2 (CP2). CP1 corresponds to stars with CCD data and is placed farther than 3.25 arcmin from the cluster centre (see Fig. 2) and covers an area similar to that of the cluster (nucleus plus corona). On the other hand, CP2 is chosen from a ring located $\sim$6.5 arcmin from the cluster centre. Examining Figs 7(c), 7(f), 8(b) and 8(c) we conclude that (i) Markarian 50 suffers from significant contamination by field stars for $V \geqslant 16$–17 and (ii) the stellar field over which we see the cluster projected against does not seem to change abruptly. As in Fig. 6, Figs 7(a), (b), (d) and (e) confirm the presence of differential reddening, which makes the cluster main sequence (MS) show a sizeable width. In all cases, it is very difficult to separate cluster from field stars because both types of star share a similar position in the diagrams (see Figs 7c and f).

3.3 Cluster memberships

To perform the membership assignment in the Markarian 50 region we combined spectroscopic data available for the brightest stars (Crampton 1975; Turner et al. 1983; Massey et al. 2001) with the classical photometric method, which relies on the comparison of
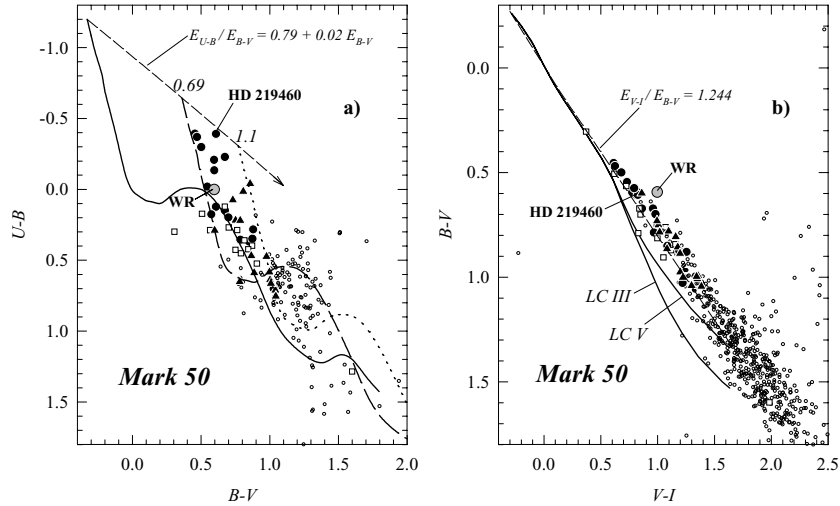
Figure 6. Colour–colour diagrams of stars placed inside the adopted radius for Markarian 50 ($R = 3.25$ arcmin). (a) (U–B) versus (B–V) diagram. Filled circles are likely members, solid triangles are probable members, open squares are non-member stars and small open circles are stars without any membership assignment. The solid line is the Schmidt-Kaler (1982) ZAMS; the dashed and dotted lines give the ZAMS shifted 0.68 and 1.1 in $E(B–V)$ (see Section 3.4). The dashed arrow points out the normal reddening path. (b) B–V versus V–I diagram. Symbols as in (a). The solid lines represent the intrinsic positions for stars of luminosity classes V and III (Cousins 1978a,b). The dashed line shows the normal reddening path ($R = 3.1$).

the star locations in all the photometric diagrams simultaneously (see, for instance, Carraro 2002; Baume et al. 2003; Baume et al. 2004). In addition, we checked the spatial star positions according to the cluster radius (see Section 3.1). This way, we recognize the following groups: likely members (lm), probable members (pm), non-members (nm) and stars without membership assignment (see photometric diagrams).

Particular cases are stars $_T$30A and $_T$31A (Turner et al. 1983 numbering) which have been separated into two pairs ($_T$30A1–$_T$30A2 and $_T$31A1–$_T$31A2, respectively) and their memberships indicated in Table 3. Star $_T$31A1 has been assumed a probable member; however, its final corrected position (see in advance Fig. 10) is slightly high above the MS. On the other hand, stars $_T$42 and $_T$58 were considered background and foreground objects, respectively, by Turner et al. (1983), but after our analysis they are adopted as pm and lm, respectively. In fact, the reddening in the north of the cluster presents higher values, which, when removed, put star $_T$58 in an acceptable position in all the diagrams.

In order to compute the cluster LF and IMF up to faint magnitudes (see Section 3.2), we estimate the amount of cluster members in the lower MS using the apparent LF of CP1 and the corresponding one in the cluster region ($R < 3.25$ arcmin). Their subtraction and a completeness analysis provide us with an estimate of the number of cluster members that must be expected (see Baume et al. 2003) along the faint part of the cluster MS. Together with the counts performed in the brighter magnitude bins among the adopted lm and pm stars, this result is presented in Table 4.

3.4 Corrected colours and magnitudes

For the stars having spectroscopic data, individual colour excesses were obtained following the relation between spectral classification and colours given by Schmidt-Kaler (1982). For lm and pm stars without spectral classification or without unique reddening solution, their colour excesses and intrinsic colours were estimated using the colour excess relation corresponding to this galactic direction [$E(U–B)/E(B–V) = 0.79 + 0.02\ E(B–V)$; Turner et al. 1983],

following the procedure given by Vázquez & Feinstein (1991) and by assuming that they are all stars of luminosity class V. This way, we found that individual $E(B–V)$ excesses for cluster members range from 0.69 to 1.1 with mean and standard deviation values of $E(B–V) = 0.86 \pm 0.13$ and $E(U–B) = 0.68 \pm 0.11$. We adopt then 0.69 as the cluster foreground excess [$E(B–V\ f)$]. In the particular case of HD 219460, we have assumed that the colour excesses of the WR star component are similar to the colour excesses individually computed for the other component of the system (B1III) indicated in Table 3.

To obtain corrected visual magnitudes, we carefully analyse the value of the ratio of total to selective absorption [$R = A_V/E(B–V)$] in the area. We applied two methods to cast light on this point. (i) First, it is well known that $E(V–R)/E(B–V)$ and $E(V–I)/E(B–V)$ are a measure of the R value (see Baume et al. 2003). Therefore, we computed the individual colour excesses $E(V–R)$ and $E(V–I)$ from the relations between $(B–V)_O$ and spectral types (Schmidt-Kaler 1982) and $(B–V)_O$ with $(V–R)_O$ and $(V–I)_O$ from Cousins (1978a,b). (ii) The second method is the colour difference method (see Fig. 9) where we used stars with spectral classification complementing our data with those of the 2MASS. Intrinsic colours were derived using Schmidt-Kaler (1982) and Ducati et al. (2001) relations of spectral types with colours. Individual and mean curves from this method have been computed and are shown in Fig. 9 together with the van de Hulst curve 15 (Johnson 1968) which has been drawn for comparison purposes.

The first method yields $R = 3.2$, while the second suggests, extrapolating the reddest part of the mean curve shown in Fig. 9, that the R value is also normal. It seems that the probable anomaly shown in Figs 6(b) and 7(d) and (e) only has to do with those bands. The coincidence of both methods leads us to conclude that $R = 3.1$ in the cluster direction. In using the colour difference method, the peculiar curves shown by stars $_T$17 and $_T$36 (showing apparent anomalous R values) are probably the result of a bad spectral type assignment given by Crampton (1975). He claims that his F-type spectra of these two stars are uncertain as they were subexposed.
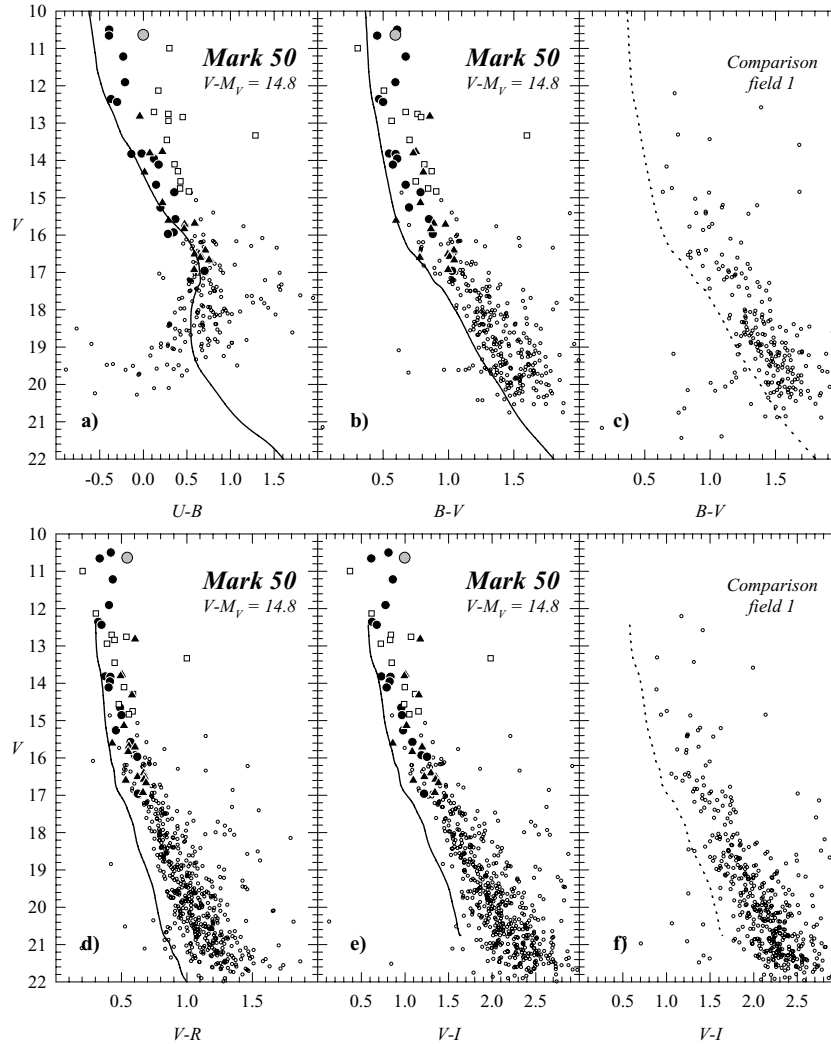
Figure 7. CMDs for nucleus + corona stars in Markarian 50 and the comparison field CP1. Symbols as in Fig. 6. The solid line is the Schmidt-Kaler (1982) ZAMS fitted to the apparent distance modulus $V - M_V$ [$= V_O - M_V + 3.1 \times E(B-V f)$; see Section 3.4]. It is also shown superposed on to the comparison fields (dotted lines).
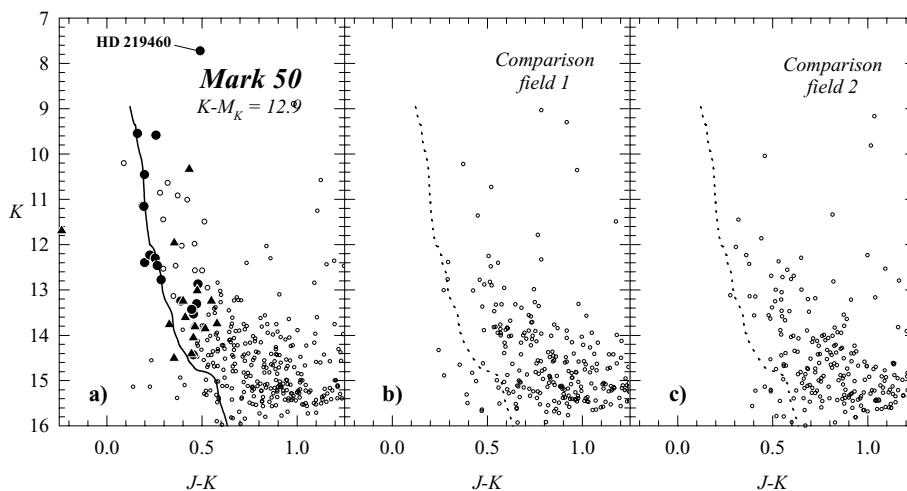
Figure 8. (a) K versus $J–K$ diagram for nucleus + corona stars in Markarian 50. Symbols as in Fig. 6. (b) K versus $J–K$ diagrams for the two comparison fields (see text). The solid line in (a) and the dotted line in (b) are the intrinsic positions for MS stars adapted from Schmidt-Kaler (1982) and Koornneef (1983) calibrations, fitted to the apparent distance modulus $K − M_K = 12.7$ [$K − M_K = V_O − M_V + 0.3 \times E(B−V)$; see Section 3.5].

Table 3. Stars in the region of Markarian 50. ₜ indicates Turner et al. (1983) numbering. Spectral classification (SC) is from Turner et al. (1983) and Massey et al. (2001). A full version of this table is available in electronic format at the WEBDA site (http://obswww.unige.ch/webda/).

| No.		2MASS ID. TYCHO ID. HD/ALS/BD ID.	X (arcsec) Y (arcsec)	α_{2000} δ_{2000}	V	$B-V$ $U-B$ $V-R$ $V-I$	$E(B-V)$ $E(U-B)$ $E(V-R)$ $E(V-I)$	SC	Memb.
1	ₜB1	J23151249 + 602701 TYC 4279-2192-1 HD 219460A	15.5 31.6	23:15:12.4 60:27:01.6	10.50	0.61 −0.39 0.42 0.81	0.87 0.61 0.53 1.10	B1 II	lm
2	ₜWR	J23151249 + 602701 TYC 4279-2192-2 HD 219460B	14.4 30.8	23:15:12.6 60:27:00.8	10.64	0.59 0.00 0.54 1.00	0.87 0.61 0.53 1.10	WN4.5	lm
3	ₜ23	J23151668 + 602607 TYC 4279-2212-1 ALS 12848	−16.1 −22.8	23:15:16.7 60:26:07.2	10.66	0.46 −0.39 0.33 0.61	0.72 0.58 0.44 0.87	B1 III	lm
4	ₜ11	J23150894 + 602516 TYC 4279-2288-1 BD + 59 2682	41.2 −73.6	23:15:08.9 60:25:16.4	10.99	0.30 0.30 0.20 0.37		A0 V	nm
5	ₜ31	J23151194 + 602646 TYC 4279-2210-1	19.0 16.5	23:15:11.9 60:26:46.5	11.22	0.67 −0.23 0.43 0.86	0.93 0.74 0.55 1.15	B0.5 II	lm
6	ₜ30A1	J23151321 + 602621	9.6 −8.4	23:15:13.2 60:26:21.6	11.91	0.59 −0.21 0.41 0.78	0.84 0.69 0.51 1.05	B1.5 V	lm
9	ₜ1	J23145990 + 602715	107.9 45.1	23:14:59.9 60:27:15.1	12.36	0.47 −0.37 0.32 0.62	0.72 0.53 0.43 0.90	B1.5 V	lm
10	ₜ30	J23151440 + 602618	0.8 −11.8	23:15:14.4 60:26:18.2	12.44	0.50 −0.30 0.35 0.68	0.74 0.54 0.45 0.94	B2 V	lm
14	ₜ42	J23151923 + 602925	−35.0 175.7	23:15:19.2 60:29:25.7	12.82	0.86 −0.04 0.60 1.18	1.12 0.91 0.72 1.46		pm
22	ₜ31A1	J23151388 + 602700	4.6 30.7	23:15:13.9 60:27:00.7	13.76	0.75 0.22 0.50 1.01			pm
23	ₜ31A2	J23151349 + 602700	7.4 29.8	23:15:13.5 60:26:59.8	13.80	0.73 0.07 0.49 0.99	0.93 0.75		pm
39	ₜ58	J23153212 + 602548	−130.5 −40.7	23:15:32.1 60:25:49.3	14.86	0.79 0.36 0.50 0.97	0.91 0.73 0.55 1.07		lm
129	ₜ30A2	J23151246 + 602625	15.1 −4.4	23:15:12.5 60:26:25.6	16.96	1.03 0.70 0.63 1.22	1.10 0.90		lm

The resulting mean optical absorption that affects Markarian 50 is ($\langle A_V \rangle = R \langle E(B-V) \rangle \approx 2.7$) entirely comparable to earlier values obtained for Cas OB2 and the region of the dust shells (Lozinskaya et al. 1986). Our value is also similar to that given by Neckel & Klare (1980) for the same Galactic direction.

3.5 Cluster distance and age

The distance of Markarian 50 has been obtained by superposing the Schmidt-Kaler (1982) zero-age main sequence (ZAMS) on to the reddening-free CMD. The best ZAMS fitting in both M_V versus

Table 4. Apparent LF.

ΔV	N	Comp.
10–11	3	100.0 per cent
11–12	2	100.0 per cent
12–13	3	100.0 per cent
13–14	5	99.8 per cent
14–15	4	99.6 per cent
15–16	9	97.0 per cent
16–17	8	95.9 per cent
17–18	10	95.7 per cent
18–19	12	89.3 per cent
19–20	22	72.4 per cent
20–21	17	58.7 per cent
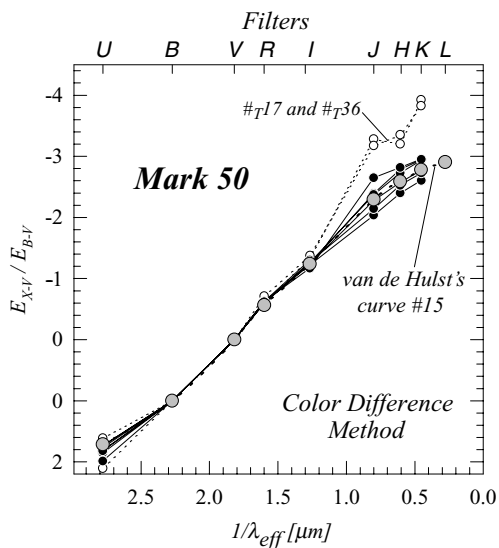
Figure 9. The colour difference method. Individual curves computed for stars with spectral classification (see Table 3) together with the extinction curve 15 from van de Hulst (slashed lines with grey symbols; Johnson 1968). Stars $_T17$ and $_T36$ are indicated (see Section 3.4).

$(U-B)_O$ and M_V versus $(B-V)_O$ was achieved for a distance modulus $V_O - M_V = 12.7 \pm 0.2$ (error from inspection). This fit is also presented in Figs 7(a), (b), (d), (e) and 8(a) using the Schmidt-Kaler (1982), Cousins (1978a), Cousins (1978b) and Koornneef (1983) calibrations for ZAMS and MS stars, shifted by the corresponding foreground colour excesses and apparent distance modulus ($V - M_V = 14.8$ or $K - M_K = 12.9$).

These distance moduli place Markarian 50 at 3460 ± 350 pc from the Sun, in the inner border of the Perseus arm, and they are in full agreement with previous distance estimates based on spectroscopic or photoelectric data (Crampton 1975; Turner et al. 1983 or Massey et al. 2001) that locate Markarian 50 at about 3.5 kpc. All these previous results, which could have been affected by uncertainty because they relied on ZAMS fittings to the vertical part of the MS of this cluster, are confirmed by our new data analysis, which assigns membership to stars 2 mag fainter than any previous works. On the other hand, it does not seem that the number of binaries in the cluster is high, as few stars are at the level of the binary envelope 0.75 mag above the ZAMS. An exception is star $_T31A1$ which rises above the ZAMS but it is still adopted as a probable member (see Section 3.3) because its position could be due to rapid rotational effects.

As for the age of Markarian 50, we also superpose in Fig. 9 the set of isochrones from Girardi et al. (2000) (computed with solar metallicity, mass loss and overshooting) on to the reddening-free CMD, finding that the most probable age of the cluster is 7.5 ± 2 Myr.

3.6 HD 219460

HD 219460 is a visual binary star composed of an evolved B-type star and a WR star of spectral types B1II and WN4.5, respectively (Turner et al. 1983). According to Marston (1996), this system is located in the centre of a shell-like structure of 27 arcmin in diameter; the nebulosity around has also been previously mentioned by Miller & Chu (1993) and Heckathorn, Bruhweiler & Gull (1982). In the VII Catalogue of WR stars (van der Hucht 2001) the system is classified as WN5 + B1II VB with absolute magnitudes of $M_V = -4.07$ for the WR star and -5.67 for the entire system. As for the period of the binary, it is uncertain, ranging from 1.786 to 2.032 (d).

Our CCD data together with the PSF technique allow us to derive individual colours and magnitudes of both components of the system. They show that the evolved B-type star is 0.14 mag brighter than the WR component, in good agreement with the earlier estimation of 0.2 mag made by Wilson (1940) and Turner et al. (1983). Van der Hucht (2001) indicates that the system is located at a distance of 2.93 kpc and suffers a visual absorption that ranges from $A_V = 2.2$ to 3.61. Although the distance value adopted by van der Hucht is smaller than ours, our estimation of the absorption of the system $[A_{V_{HD}} = 3.1E(B-V_{HD}) = 2.7]$ is consistent with the range derived above for the cluster.

With this absorption and at the cluster distance, the absolute magnitude of the WR star is $M_V = -4.75$, entirely similar to the magnitude derived by Turner et al. (1983), $M_V = -4.85$. Although this magnitude is brighter than the mean of $M_V = -4.05 \pm 1$ given by van der Hucht (2001) for a WR of this type, it is still in reasonable agreement, taking into account the magnitude dispersion quoted by van der Hucht. The agreement improves if we consider that the distance modulus of Markarian 50 shows a probable error of 0.2 mag and that Turner et al. (1983) claim that this WR star could be a variable; therefore, the different absolute magnitude value found in the present work may not be significant.

If the reddening affecting the other component of the system is assumed valid for this WN 4.5 star, then its intrinsic colours are $(B-V)_O = -0.27$ and $(U-B)_O = -0.61$. The derived $(B-V)_O$ is bluer than the most probable intrinsic $(B-V)$ value for a WR of this type, which should be $(B-V)_O = -0.22$ following Lundström & Stenholm (1984). Unfortunately, as intrinsic colours derived from broad-band photometry are, in most of the cases, meaningless for WR-type stars (due to the presence of strong emission lines) we cannot establish any clear connection with the probable optical thickness of the wind (a measure of the extension of the stellar envelope) as indicated by Smith & Maeder (1998).

An attempt has also been made to estimate the mass of the WR. Assuming it is the most evolved member of the cluster, the lower mass limit of its progenitor should be, at least, the mass of the brightest cluster stars yet on the cluster MS. A simple calculation (see the next section) yields that the mass of the brightest star yet on the MS is ~ 20 M$_\odot$. Although this value is similar to that obtained by Massey et al. (2001), it does not contradict the previous estimate made by Turner et al. (1983), who found ~ 30 M$_\odot$ using the Sreenivasan & Wilson (1982) models of binary star evolution, as the value obtained in this paper should be assumed just as a lower mass limit.
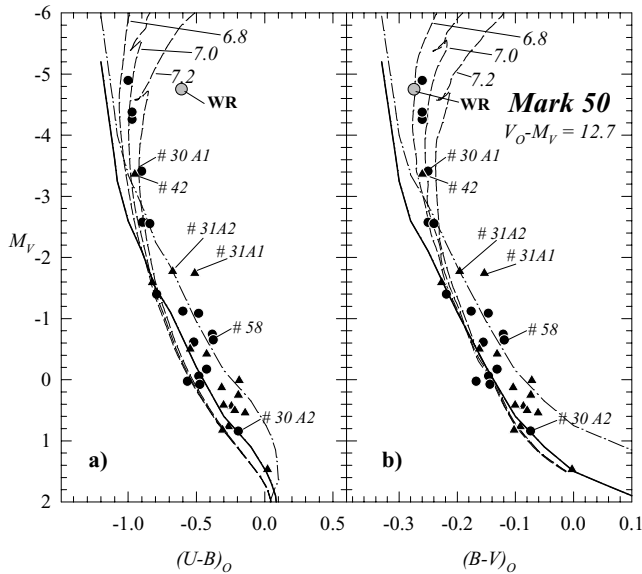
Figure 10. The M_V versus $(U-B)_O$ and $(B-V)_O$ diagrams. Symbols as in Fig. 6(a). The solid line is the Schmidt-Kaler (1982) ZAMS. Dashed lines are the isochrones from Girardi et al. (2000). Numbers give the log(age). The dot-dashed line represents the binary envelope 0.75 mag above the ZAMS. Stellar identifications are according to Turner et al. (1983) numbering.
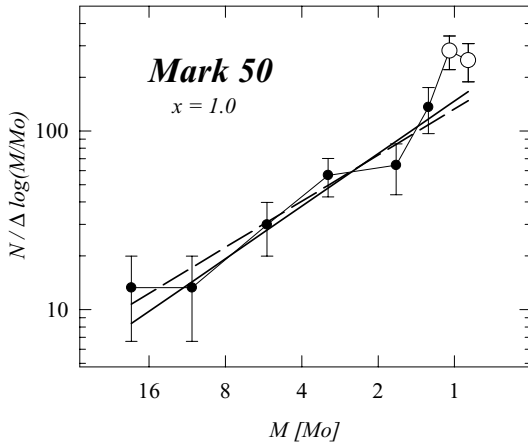
Figure 11. IMF for Markarian 50. Error bars are from Poisson statistics. The weighted least-squares fits for more massive bins are indicated with solid and dashed straight lines (open symbols indicate bins not included in the fits). See text for more details.

3.7 Initial mass function

The IMF gives the number of stars formed over the mass interval at the same time in a given region of space (Scalo 1986). In this case, we superimpose on to the corrected CMDs (not shown in Fig. 10 for clarity) the tracks for the previously used evolutionary models of Girardi et al. (2000) and from them we interpolate the corresponding individual stellar masses. This procedure was applied for the brightest cluster stars. As usual in these cases, the WR star was included in the most massive bin, given its evolved nature. As for the lower MS stars of Markarian 50 ($V > 17$), we use the apparent LF of Table 4, obtaining the absolute magnitudes through the apparent distance modulus and computing the corresponding masses from the mass–luminosity relation given by Scalo (1986). The results are presented in Fig. 11, where a weighted least-squares fitting is

performed for the most massive bins ($M > 1.1$ M$_{\odot}$), obtaining a slope value $x = 0.86 \pm 0.11$ (dashed line). If the most massive bin is not taken into account (in order to minimize the influence of the probable presence of binary stars) the slope slightly changes reaching $x = 0.98 \pm 0.13$ (solid line).

4 DISCUSSION AND CONCLUSIONS

Markarian 50 is a young open cluster which harbours a WR star, probably the main cause of the nebula around it. Knowledge of the cluster fundamental parameters (such as distance and age) and, consequently, the intrinsic parameters of its WR star may help to understand their nature and the relationship with the molecular complex lying near them, as well as with all other structures of this region of the Perseus arm.

In this paper we present the first deep CCD observations of the region of this cluster in order to compare earlier results with those from our new data set. In this respect we have found that the cluster is placed at about $d = 3460$ pc from the Sun in the inner part of the Perseus arm; from the fitting to modern isochrones, we have estimated that its age is near to 7.5 Myr. These results, including the reddening estimation, confirm previous values derived by Turner et al. (1983).

Our improved estimates of the cluster age and distance provide hints to the possible scheme of star formation on a large scale in this region of the Perseus arm. A possible cascade scenario of formation was presented by Lozinskaya et al. (1986) that involves the association Cas OB2, the open cluster NGC 7510 (Barbon & Hassan 1996) and Markarian 50, in this order. The following step would be the compact H II region Sh 2–157A placed nearly 0°5 southward of Markarian 50. Our distance estimation (3.46 Kpc) locates Markarian 50 not so far from NGC 7510, placed at 3.2 Kpc (Sagar & Griffiths 1991) or 3.09 Kpc (Barbon & Hassan 1996). This fact corroborates the idea of the cascade scenario mentioned above.

Figs 4 and 5 together with the analysis presented in Section 3.1 confirm that Markarian 50 presents a nucleus/corona structure with radii of 1.25 and 3.25 arcmin, respectively. This is an interesting fact because for a cluster as young as Markarian 50 this type of structure cannot be ascribed to dynamical evolution but should be an imprint of the star formation process in this region. A similar scenario is present in other young clusters such as Trumpler 14 (Vázquez et al. 1996).

According to Salpeter (1955), a typical value for the IMF slope is $x = 1.35$, but it is widely argued that it is only a sort of reference value, as many claims have been made for an environmental dependence of the mass function (Scalo 1998). In the present case, the slope value is significantly lower than that of Salpeter, but it is still similar to those obtained in previous analysis of other young open clusters such as Trumpler 14 (Vázquez et al. 1996), NGC 6231 (Baume, Vázquez & Feinstein 1999), H-M 1 (Vázquez & Baume 2001), IC 1590 (Guetter & Turner 1997) or the young region Cyg OB2 (Massey & Thompson 1991). This way, we see a type of trend in the sense that the flatter the IMF slopes, the younger the open clusters and associations. This fact could indicate that an earlier cluster dissolution would affect the value of the IMF slope, a result that should be addressed in more detail by enlarging the sample of young cluster IMFs.

ACKNOWLEDGMENTS

This paper is partially based on the DSS-2 that was produced at the Space Telescope Science Institute under US government

REFERENCES

Barbon R., Hassan S. M., 1996, A&AS, 115, 325
Baume G., Vázquez R. A., Feinstein A., 1999, A&AS, 137, 233
Baume G., Vázquez R. A., Carraro G., Feinstein A., 2003, A&A, 402, 549
Baume G., Moitinho A., Giorgi E. E., Carraro G., Vázquez R. A., 2004, A&A, 417, 961
Caldwell J. A. R., Cousins A. W. J., Ahlers C. C., van Wamelen P., Maritz E. J., 1993, SAAO Circ., 15, 1
Carraro G., 2002, MNRAS, 331, 785
Cousins A. W. J., 1978a, Mon. Notes Astron. Soc. S. Afr., 37, 62
Cousins A. W. J., 1978b, Mon. Notes Astron. Soc. S. Afr., 37, 77
Crampton D., 1975, PASP, 87, 523
Desidera S., Fantinel D., Giro E., 2002, AFOSC User Manual
Dias W. S., Alessi B. S., Moitinho A., Lépine J. R. D., 2002, A&A, 389, 871
Ducati J. R., Bevilacqua C. M., Rembold S. B., Ribeiro D., 2001, ApJ, 558, 309
Forbes D., 1996, AJ, 112, 1073
Girardi L., Bressan A., Bertelli G., Chiosi C., 2000, A&AS, 141, 371
Grubissich C., 1965, Zeitschrift für Astrophys., 60, 249
Guetter, Turner, 1997, AJ, 113, 2116
Heckathorn J. N., Bruhweiler F. C., Gull T. R., 1982, ApJ, 252, 230
Johnson H. L., 1968, in Middlehursst B. M., Aller L., eds, Nebulae and Interstellar Matter. Univ. Chicago Press, p. 167
Koornneef J., 1983, A&A, 128, 84
Landolt A., 1992, AJ, 104, 30
Lozinskaya T. A., Sitnik T. G., Lomovskii I., 1986, Ap&SS, 121, 357
Lundström I., Stenholm B., 1984, A&AS, 58, 163
Lyngå G., 1987, Catalogue of Open Star Cluster Data. CDS, Strasbourg
Marston A. P., 1996, AJ, 112, 2828
Massey P., Thompson A. B., 1991, AJ, 101, 1408
Massey P., DeGioia-Eastwood K., Waterhouse E., 2001, ApJ, 121, 1050
Miller G. E., Scalo J. M., 1979, ApJS, 41, 513
Miller G. J., Chu Y.-H., 1993, ApJS, 85, 137
Neckel Th., Klare G., 1980, A&AS, 42, 251
Sagar R., Griffiths W. K., 1991, MNRAS, 250, 683
Salpeter E. E., 1955, ApJ, 121, 161
Scalo J., 1986, Fundam. Cosmic Phys., 11, 1
Scalo J., 1998, in ASP Conf. Ser. Vol. 142, The Stellar Initial Mass Function, 38th Herstmonceux Conference. Astron. Soc. Pac., San Francisco, p. 201
Schmidt-Kaler Th., 1982, in Schaifers K., Voigt H. H., eds, Landolt–Börnstein, Numerical Data and Functional Relationships in Science and Technology, New Series, Group VI, Vol. 2(b). Springer Verlag, Berlin, p. 14
Shorlin S. L., Turner D. G., Pedreros M. H., 2004, PASP, 116, 170
Smith L. F., Maeder A., 1998, A&A, 334, 845
Sreenivasan S. R., Wilson W. J. F., 1982, ApJ, 254, 287
Stetson P. B., 1987, PASP, 99, 191
Turner D. G., Moffat A. F. J., Lamontagne R., Maitzen H. M., 1983, AJ, 88, 1199
van der Hucht K. A., 2001, New Astron. Rev., 43, 135
Vázquez R. A., Baume G., 2001, A&A, 371, 908
Vázquez R. A., Feinstein A., 1991, A&AS, 90, 317
Vázquez R. A., Baume G., Feinstein A., Prado P., 1996, A&AS, 116, 75
Will J.-M., Bomans D. J., de Boer K. S., 1995, A&A, 295, 54
Wilson O. C., 1940, PASP, 52, 404

This paper has been typeset from a TEX/LATEX file prepared by the author.